

# Crystallization Improvements of a Diastereomeric Kinetic Resolution through Understanding of Secondary Nucleation

Patrick Mousaw,\* Kostas Saranteas, and Bob Prytko

Chemistry &amp; Pharmaceutical Sciences, Sepracor Inc., 84 Waterford Drive, Marlborough, Massachusetts 01752, U.S.A.

## Abstract:

The crystallization of a diastereomeric kinetic resolution was studied as part of a continuous process improvement initiative. The isolated intermediate was failing optical purity specifications at a contract manufacturing site. These failed batches also exhibited longer filtration and drying times. Experimentation studied the significant secondary nucleation event observed during the process. By using the secondary nucleation induction temperature as the response variable, the shear rate introduced by the impeller and seed surface area were identified as the critical process parameters that significantly influence this significant secondary nucleation event. Scale-up implementation of the laboratory findings led to a more robust resolution process with no optical purity failure reported with well over 50 commercial batches executed. The results from the experimental studies are compared to those from various mechanistic models available in the literature.

## Introduction

The isolation of single enantiomers from racemic mixtures in high purity has become increasingly more common in the pharmaceutical industry. There are several reasons for this trend. If it is possible to isolate the enantiomer with the desired biological activity, it may be possible to eliminate undesirable side effects associated with the other isomer. The FDA has been encouraging companies to submit applications of highly pure active single isomers rather than racemic mixtures.<sup>1</sup>

One method of separating an enantiomer in high purity from a racemic mixture is through diastereomeric resolution. This process involves reacting the racemic mixture with a resolving agent, which is an enantiomerically pure acid or base, to form a mixture of diastereomers that, by definition, exhibit different solubilities and thus can be separated by traditional crystallization procedures.<sup>2</sup> In an ideal system, the desirable diastereomer is both kinetically and thermodynamically favorable. However, it is also possible for one diastereomer to be kinetically favored while the other diastereomer is thermodynamically favored. For the latter case, the crystallization conditions can play a major role in the performance of the resolution.

A two-step resolution process was developed, scaled-up, and validated at a contract manufacturer site that involved a diastereomeric resolution step followed by a free-basing step

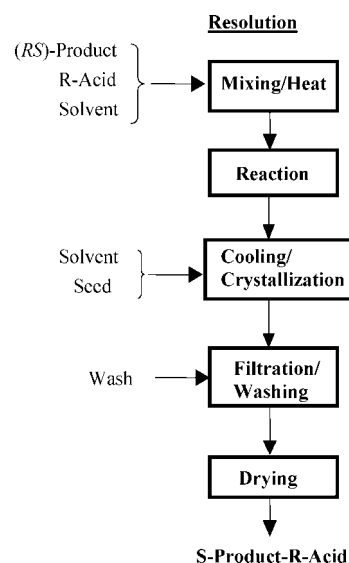


Figure 1. Block flow diagram of the resolution process.

that yielded the (*S*)-enantiomer free base as the final API, as shown in Figure 1. Upon commercialization of the process, the diastereomeric resolution manufacturing step was characterized by periodic quality specification failures in terms of enantiomeric purity (i.e., high levels of (*R*)-enantiomer). In addition, this intermediate step was characterized by long and variable filtration and drying steps that caused significant productivity drop at the manufacturing site.

The large batch-to-batch variability in the intermediate step prompted several strategies. Early on in the development program, a rework procedure was developed and validated on full scale as a back-up option to address failed batches and ensure a reproducible high-quality API production. Additionally, studies focusing on the seeding and cooling operation were performed because of observations noting differences in the crystallization profile from batch-to-batch. The work reported here is part of a continuous process improvement initiative to address the robustness and productivity of the commercialized process.

**Solubilities and Metastable Zone Mapping.** The solubilities of Diastereomer A (*S*-isomer) and Diastereomer B (*R*-isomer) were tested in the solvent system selected for the resolution. This testing occurred at two different sites and produced very similar results. The solubility of Diastereomer A in the selected solvent system is always greater than the solubility of Diastereomer B over the temperature range of interest (Figure 2). Diastereomer A, the desired product, is the kinetically favored, whereas Diastereomer B, the undesired

\* Author for correspondence. E-mail: pmousaw@nd.edu.

(1) FDA'S Policy Statement for the Development of New Stereoisomeric Drugs. <http://www.fda.gov/cder/guidance/stereo.htm5/1/1992>.

(2) Mersmann, A. *Crystallization Technology Handbook*; Marcel Dekker, Inc: New York, 1995; pp 417–418..

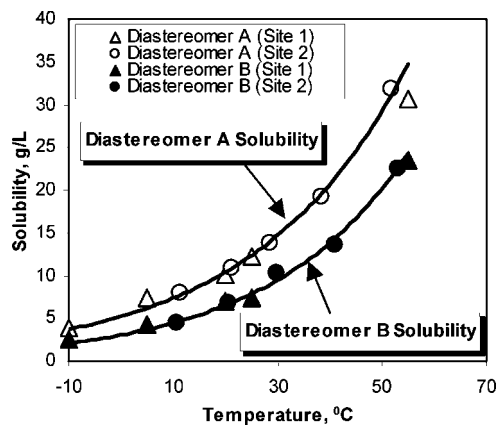


**Figure 2.** Solubility of Diastereomer A and Diastereomer B in selected solvent system.

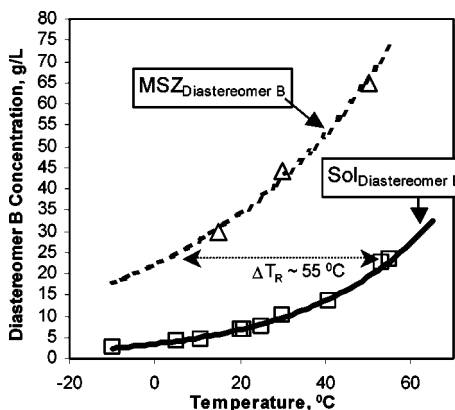


**Figure 3.** Solubility and metastable zone of Diastereomer B in selected solvent system.

product, is thermodynamically favored. An estimation of the metastable zone of Diastereomer B was also experimentally determined.

A comparison of the solubility and metastable zone of Diastereomer B shows that there is a wide temperature differential between the two curves. Specifically, at the concentration of interest, there is a temperature differential of around 55 °C (Figure 3). This large temperature differential allows for the isolation of Diastereomer A without spontaneously nucleating Diastereomer B. The solubilities and Diastereomer B metastable zone offer some potential explanations of the observed quality failures of the step (kinetic- rather than thermodynamic-based resolution). Focus then shifted to the evaluation of the seeded cooling crystallization step as a potential source of the observed quality variability.

**Seeding and Secondary Nucleation Analysis.** An operation that improves the performance of a kinetic resolution is seeding with the desired diastereomer. The seeding operation provides a surface for the selective growth of the desired diastereomer and suppresses the nucleation of the undesired diastereomer. Similar to achiral systems, seeding also helps to minimize secondary nucleation and leads to larger crystals and fewer fines.

Modifying the seeding operation in the process producing Diastereomer A was initially pursued as a means for promoting crystal growth and eliminating an aggressive nucleation event identified in the original seeding protocol. However, while

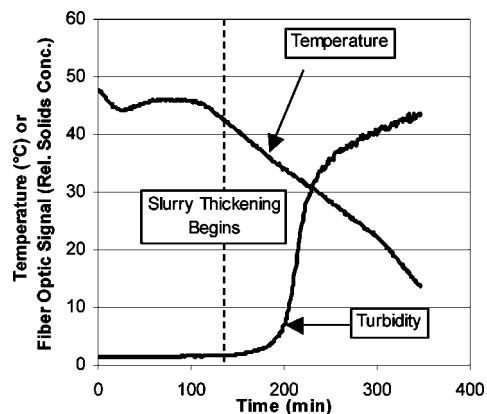


**Figure 4.** Example of the fiber-optic turbidity probe detecting the slurry density.

conducting experiments towards these goals, it became clear that suppressing the aggressive nucleation event by slowing down the cooling step would be very challenging. Fortunately, the role of seeding was found to be very important to the nature of the nucleation event, as discussed below.

In the originally developed process for producing Diastereomer A, a seeding operation was specified at a batch temperature of 46 °C and seed loading of 0.2 wt %. After seeding, the batch is cooled to 12 °C over 4 h in three linear steps. Visually, the slurry typically becomes thicker about 1 to 2 h after the seeding operation takes place. Data from the Lasentec FBRM probe<sup>3,4</sup> at laboratory scale and from an *in situ* fiber-optic turbidity probe at manufacturing scale show the slurry density changes very little before the slurry becomes visually thicker. Figure 4 shows an example profile.

Immediately preceding being able to visually see the thickening of the slurry, both the Lasentec FBRM and the fiber-optic data show a sharp and sudden increase in particle counts or slurry density. The temperature at which this sharp increase started was termed the secondary nucleation induction temperature, or  $T_N$ . The data from the *in situ* turbidity probe was collected for all the batches of one campaign at the contract manufacturer. This campaign data showed that batches with higher  $T_N$ 's produced Diastereomer A with less Diastereomer B impurity and took less time to process, as shown by Figure 5.

A semiempirical correlation for the secondary nucleation rate is given as follows:<sup>5-7</sup>

$$B_s \approx k_n A^i M_T^j S^b \quad (1)$$

where  $B_s$  = number of nuclei/unit time/unit volume;  $k_n$  = temperature-dependent rate constant;  $A$  = agitation rate or equivalent;  $M_T$  = suspension density (mass of crystals per unit

- (3) Barrett, P.; Glennon, B. *Part. Part. Syst. Charact.* **1999**, *16*, 207.
- (4) Worlitschek, J.; Mazzotti, M. *Part. Part. Syst. Charact.* **2003**, *20*, 12-17.
- (5) Tavaré, N. *Industrial Crystallization: Process Simulation Analysis and Design*; Plenum Press: New York 1995; pp 64-65.
- (6) Jones, A. G. *Crystallization Process Systems*; Butterworth-Heinemann: Oxford, 2002; p 150.
- (7) Genck, W. Crystallization - Part 1. *Chem. Process.* **2003**, (October), 63.

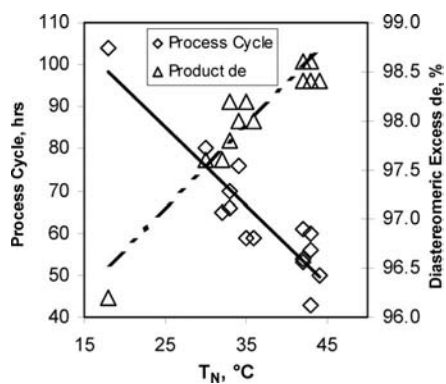


**Figure 5.** Process cycle time and product Diastereomer A purity versus  $T_N$ .

volume);  $S$  = supersaturation;  $i, j, b$  = experimentally determined power constants.

While eq 1 provides a qualitative relationship between nucleation rate and seed mass or mixing it is clearly not adequate to explain some of the experimental results obtained. Additional models have been proposed in literature<sup>8–11</sup> discussing surface-versus contact-based secondary nucleation mechanisms, but they fail to explain optical purity effects of seeding.

**Identifying the Secondary Nucleation Induction Temperature.** By using the Lasentec FBRM probe, the temperature at which the secondary nucleation event takes place can be estimated. The actual temperature identified can vary quite a bit, depending on what method is used to identify the start of the secondary nucleation event. A systematic approach was needed to have consistent estimations of the temperature at which the event occurred.

The method chosen to estimate the  $T_N$  was the first derivative of the counts per second in the range of 1–1000  $\mu\text{m}$ , as measured by the FBRM. Figure 6 shows an example of such a profile. The initial positive slope observed is the result of the seeding operation. The start of the subsequent sharp and sudden increase in slope is the time point at which the corresponding temperature represents the  $T_N$ .

**Effect of Mixing.** One factor in eq 1 is a measure of mixing. An experimental strategy was used that is similar to what was outlined by Genck in the December 2003 issue of *Chemical Processing*.<sup>12</sup> Experiments were conducted in a 1-L cylindrical jacketed bottom-valve vessel with either a pitch blade or retreat curve agitator. The experiments were seeded with a 0.2 wt % seed loading. The agitation rate was varied between experiments and the corresponding  $T_N$  recorded.

Several scale-up mixing parameter estimates based on agitator speed, agitator type, reactor geometry, and fill volume were made using VisiMix software.<sup>13</sup> The mixing parameters

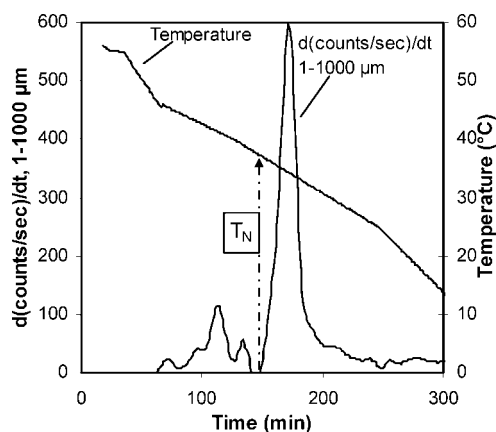


**Figure 6.** First derivative profile of counts/s (1–1000  $\mu\text{m}$ ) by FBRM and temperature profile.

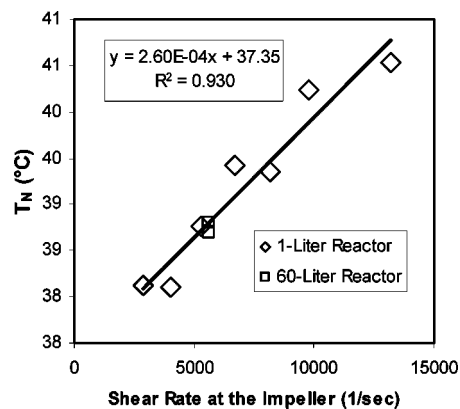


**Figure 7.** Experimental results for the  $T_N$  at different shear rates in two different sized vessels.

estimated were mixing power, tip speed, energy of dissipation at the impeller, and shear rate at the impeller. The VisiMix software does not include the effects of crystals in the fluid. However, the crystal density in this system is very dilute compared to typical pharmaceutical crystallization systems. Therefore, the effect of crystal density was assumed to be negligible.

Based on experimental results at the 1-L scale, both tip speed and shear rate at the impeller appeared to be decent fits. This was determined by doing a linear least-squares fit on the experimental results versus the mixing parameter estimates and evaluating the resulting goodness of fit, or  $R^2$ . After incorporating data from two runs in a 60-L kilo laboratory vessel, the shear rate at the impeller proved to be an appropriate mixing parameter estimate for eq 1. Figure 7 summarizes the  $T_N$  from these experiments versus estimated shear rate in the vessel used.

Figure 8 shows the estimated shear rate at the impeller versus agitation in different vessels, as determined by VisiMix. Assuming a similar cooling profile, seed load, and seed type, the appropriate agitation to achieve a  $T_N$  as determined experimentally in 1- and 60-L vessels can be quickly determined for these other sized vessels, which represent vessels used to manufacture this intermediate.

**Effect of Seeding.** Another factor in eq 1 is the slurry density. The equation suggests that an equal mass of seed per unit volume at the same temperature and supersaturation using the same agitation will promote the same secondary nucleation

- (8) Wakao, H.; Hiraguchi, H.; Ishii, T. *Chem. Eng. J.* **1987**, *35*, 169.
- (9) Daudey, P. J.; Van Rosmalen, G. M.; De Jong, E. J. *J. Cryst. Growth*. **1990**, *99*, 1076.
- (10) Togkalidou, T.; Tung, H.-H.; Sun, Y.; Andrews, A. T.; Braatz, R. D. *Ind. Eng. Chem. Res.* **2004**, *43*, 6168.
- (11) Oullion, M.; Puel, F.; Fevotte, G.; Righini, S.; Carvin, P. *Chem. Eng. Sci.* **2007**, *62*, 833.
- (12) Genck, W. Scale Up, Simulation and New Technologies - Part 2. *Chem. Process.* **2003**, (December), 37.
- (13) VisiMix Turbulent, VisiMix Ltd., Jerusalem, Israel, 2000. <http://www.visimix.com>.

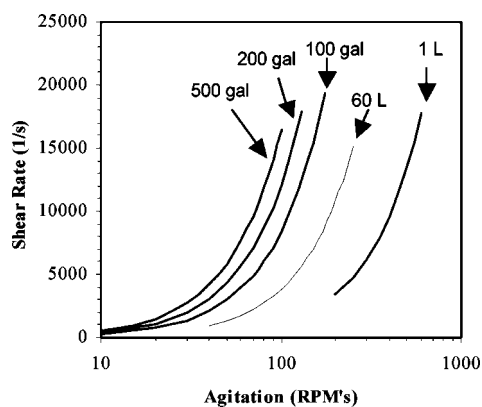


**Figure 8.** Shear rate at the impeller in various vessels, varying agitation, as determined by VisiMix.

**Table 1.** Experimental summary using seed lots with different surface areas

| experiment | seed amt. (%) | seed SSA <sup>a</sup> (m <sup>2</sup> /g) | T <sub>N</sub> (°C) |
|------------|---------------|---|---------------------|
| 1          | 0.2           | 4.44                                      | 36.8                |
| 2          | 0.2           | 4.44                                      | 36.9                |
| 3          | 0.2           | 4.44                                      | 38.3                |
| 4          | 0.2           | 4.44                                      | 37.6                |
| 5          | 0.2           | 0.42                                      | 32.6                |
| 6          | 2.0           | 0.42                                      | 38.8                |

<sup>a</sup> SSA = specific surface area.

rate. Applied to the resolution being discussed, this should also produce the same  $T_N$  and rate. However, experimentation suggests a different relationship.

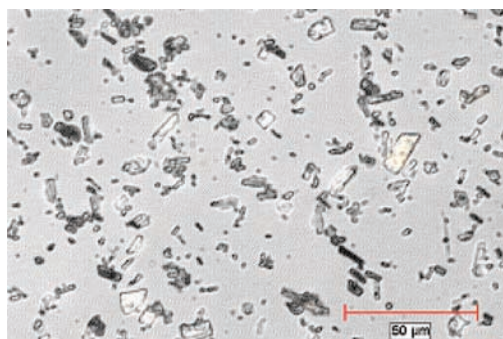
A set of experiments was executed using seeds from one of two lots. The major difference between the seeds was the specific surface area of those seeds. The first lot had a specific surface area of 4.44 m<sup>2</sup>/g, while the second lot had an area of about 1/10 of that at 0.42 m<sup>2</sup>/g. In all the experiments, the agitation, initial concentration, and cooling temperature profile were kept constant. Seeding was performed at either 0.2 wt % or 2.0 wt %.

Table 1 summarizes the results from the experiments. Experiments 1–4 show that using 0.2 wt % seed load with 4.44 m<sup>2</sup>/g specific surface area produces a  $T_N$  between 36.8 and 38.3 °C. Using seeds of 1/10 the specific surface area at 0.2 wt % load depressed the  $T_N$  to 32.6 °C, as shown by experiment 5. Experiment 6 used 2.0 wt % seed load of the seeds with 0.42 m<sup>2</sup>/g specific surface area. This experiment shows that charging roughly the same total surface area (10× the other seeding amount with 1/10 the surface area) produces a very similar  $T_N$  to those of the first four experiments at 38.8 °C.

The results of the experiments suggest that the total surface area rather than the slurry density is the important factor in  $T_N$ .

#### Effect on Particle Size, Filtration, and Optical Purity.

As already discussed, the seeding and agitation conditions have a significant impact on the  $T_N$ . Other factors affected by seeding and agitation are particle size, filtration, and optical purity. Higher seeding amounts and agitations produce crystalline solids with fewer agglomerates and longer, wider needles. As a result of higher seeding and agitation, the solids filter better and have improved optical purities. Although no quantitative particle size differences were measured between low seeding and agitation



**Figure 9.** Microscopy of manufacturing run of original process.

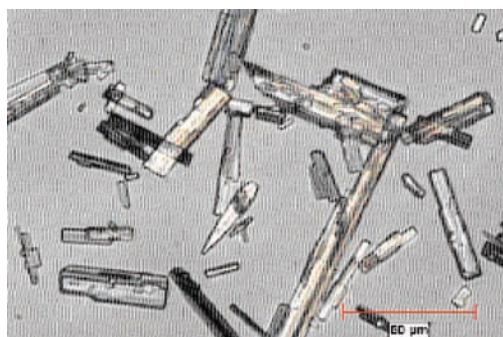


**Figure 10.** Microscopy of manufacturing run of 10× seeding process.

lots versus high seeding and agitation lots, the qualitative differences are shown by microscopy in Figures 9 and 10, which are from two manufacturing lots.

Figure 11 shows the differences in crystallization profiles between two runs during a screening DOE that screened a range of process parameters and evaluated the responses of the  $T_N$ , enantiomeric excess ( $ee_s$ ), and filtration time ( $t_{fil}$ ). Experiments with high  $T_N$ , as in experiment 1, produced solids with faster filtration rates and better optical purities than those with low  $T_N$ , as in experiment 2 (a 30-s filtration and 99.1%  $ee_s$  for  $T_N = 43.5$  °C versus a 150-s filtration and 85.7%  $ee_s$  for  $T_N = 18.0$  °C).

A higher  $T_N$  allows for a shorter nucleation event, producing fewer nuclei. As a result, a longer growth event occurs on these fewer nuclei and promotes larger, less agglomerated crystals. This produces faster filtration with better mother liquor removal, resulting in better optical purity. The effects of seeding on product quality attributes are also summarized in Figure 12.

#### Discussion of Experimental Findings

The experimentation found the agitation shear rate at the impeller and the total seed surface area to be the most significant factors affecting the secondary nucleation induction temperature,  $T_N$ , and the optical purity of the isolated diastereomer. Unfortunately, no single semi-empirical model identified in the literature is adequate to explain all of the experimental findings. The semi-empirical model introduced in eq 1 supports the effect of shear rate. The surface area effect is captured in other semi-empirical models, as referenced above. The optical purity effect

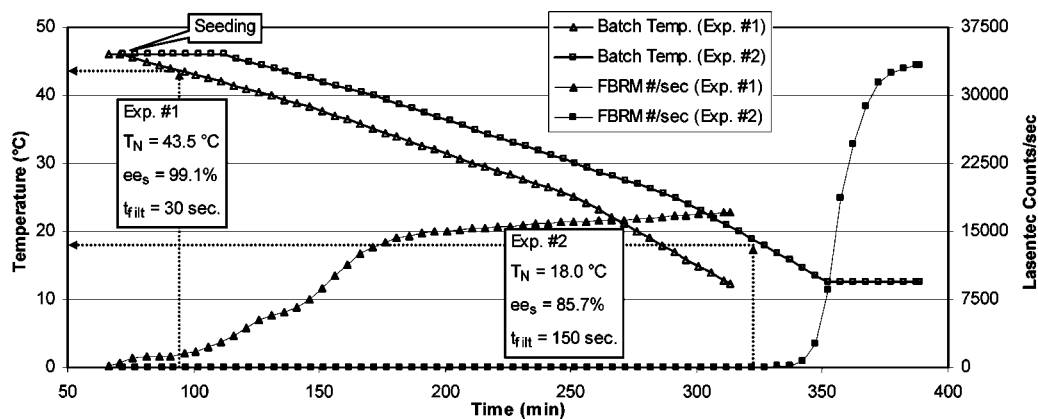


Figure 11. Crystallization profiles for two experiments using different seeding and agitation conditions.

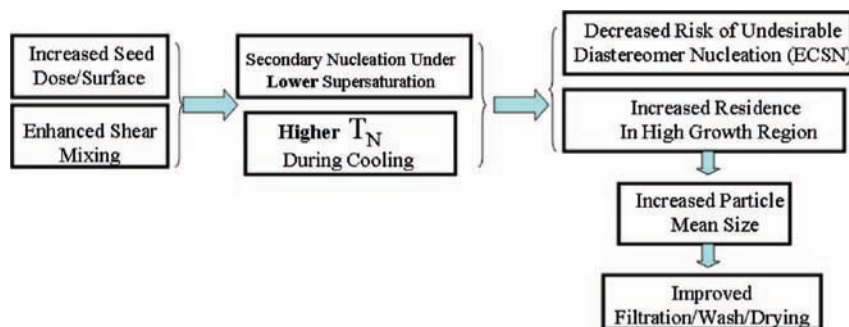


Figure 12. Effect of seeding improvements on product quality attributes.

Table 2. Kilo-laboratory filtration and  $T_N$  results on original and  $10\times$  seeding processes

| batch | seed amt. (wt %) | agitation (RPMs) | filt. time (min) |
|-------|------------------|------------------|------------------|
| 1     | 0.2              | 131              | 10.5             |
| 2     | 2.0              | 131              | 6.5              |
| 3     | 2.0              | 234              | 6                |
| 4     | 2.0              | 131              | 4                |
| 5     | 2.0              | 234              | 4                |
| 6     | 0.2              | 131              | 11               |

Table 3. Process validation at contract manufacturer in 2006

| parameter   | original                        | $10\times$ seeding              |
|---|---------------------------------|---------------------------------|
| secondary nucleation induction temperature              | average: 37 °C; range: 26–43 °C | average: 44 °C; range: 42–45 °C |
| centrifugation time                                     | average: 7.5 h; range: 3–12 h   | average: 2.2 h; range: 1–4 h    |
| manual discharge of centrifuge required?                | yes                             | no                              |
| no. of failed batches ÷ no. of batches in 2006 campaign | 3/18                            | 0/39                            |

is supported by a secondary nucleation model proposed by Qian and Botsaris called embryos coagulation secondary nucleation (ECSN).<sup>14,15</sup>

**Scale-Up Implementation Summary.** The laboratory findings of potential improvement in the diastereomeric resolution step on quality, filterability and robustness were demonstrated in scale-up campaigns in the kilo-laboratory (50 L) and the pilot plant (400 L) scale. Table 2 shows the filtration and  $T_N$  results collected at kilo-laboratory scale. The seeds came from the same lot for all batches, with batches 4 and 5 using a portion of the seed batch that had been milled to increase the seed specific surface area. The agitation levels were chosen to obtain a large difference in shear rates, with the higher level representing proposed manufacturing operation conditions.

Running at  $10\times$  the seeding amount provided a significant improvement in  $T_N$  and cut the filtration time roughly in half-compared to running the original process conditions. Also, the higher agitation batches produced a  $T_N$  that was about 2 °C higher than the lower agitation batches of the 2 wt % seed load.

(14) Qian, R. Y.; Botsaris, G. D. *Chem. Eng. Sci.* **1997**, *52*, 3429.

(15) Qian, R. Y.; Botsaris, G. D. *Chem. Eng. Sci.* **1998**, *53*, 1745.

The internal scale-up findings were communicated to the manufacturing site partner and the suggested improvements were demonstrated during dedicated demonstration campaigns with significant improvements reported, as summarized in Table 3. Specifically, four readily apparent improvements in operation were apparent. First, the  $T_N$ , as detected by the *in situ* turbidity probe, was consistently reproduced at levels above 40 °C. Second, the centrifugation operation time was reduced to an average of about 2 h. Also, the product did not require an operator to scrape it out of the tumble dryer. Additionally, the amount of Diastereomer B was consistently low in the isolated Diastereomer A, and well below the release specification for the off diastereomer. Figures 9 and 10 show the resulting crystals from the original and  $10\times$  seeding processes, respectively. The  $10\times$  seeding process produces larger crystals with fewer fines compared to the original process. During the campaign in which this  $10\times$  increase in seeding was implemented, 18 batches were operated at the original seed load of 0.2 wt % and experienced three failures due to high off-

diastereomer content. In contrast, 39 batches were operated at the 10× increase in seeding (2.0 wt %), and zero failures occurred.

## Conclusions

Controlling the induction point of the secondary nucleation event in this diastereomeric kinetic resolution using mixing- and seeding-type adjustments was demonstrated. The  $T_N$  was identified as the response variable of interest and a methodology of determining this value was established. This methodology could potentially be used to characterize other crystallization systems where a large secondary nucleation event takes place. The shear rate at the impeller and the total area of the seeds charge were identified as the most important factors affecting the  $T_N$ . These findings were compared to several semi-empirical nucleation models in the literature. The shear rate was modeled in different reactors and used to give the contract manufacturing site an estimate for the equivalent agitation rate.

Increases to the shear rate at the impeller and seeding amount, thus total seed area, were implemented at the manufacturing site and produced many measurable improvements; The centrifugation and drying operations were drastically improved, resulting in considerably lower cycle times; The off diastereomer content (Diastereomer B) in the isolated Diaste-

reomer A were consistently well below the release specifications. The robustness of the process also appears to be improved: in 2006, 39 batches under these conditions were operated with zero failures, while 18 batches were operated using the original conditions with three failures.

## NOMENCLATURE

|            |   |
|------------|---|
| $10\times$ | 10 times  |
| $A$        | agitation rate or equivalent                          |
| $b$        | experimentally determined power constant              |
| $B_s$      | number of nuclei/unit time/unit volume                |
| $i$        | experimentally determined power constant              |
| $j$        | experimentally determined power constant              |
| $k_n$      | experimentally determined power constant              |
| $M_T$      | suspension density (mass of crystals per unit volume) |
| $S$        | supersaturation                                       |
| $T_N$      | secondary nucleation induction temperature            |

Received for review November 30, 2007.

OP700276W